CONF-8309161--1

PNL-SA-11544

DISCLAIMER

PREPARATION AND PROPERTIES OF ELECTRICALLY CONDUCTING CERAMICS BASED ON INDIUM OXIDE-RARE EARTH OXIDES-HAFNIUM OXIDES

D. D. Marchant
J. L. Bates

PNL-SA--11544

DE84 000150

September 1983

Presented at the Symposium on High Temperature Solid Oxide Electrolytes
Meeting in Upton, NY
September 16-18, 1983

Supported by
the U.S. Deaprtment of Energy
under Contract DE-AC06-76RLO 1830

Pacific Northwest Laboratory
Richland, Washington 99352

MASTER

DISCLAIMER

PNL-SA-11544

PREPARATION AND PROPERTIES OF ELECTRICALLY CONDUCTING CERAMICS BASED ON INDIUM OXIDE-RARE EARTH OXIDES-HAFNIUM OXIDE

D. D. Marchant and J. L. Bates
Materials Department
Pacific Northwest Laboratory(a)
Richland, Washington 99352

ABSTRACT

Electrically conducting refractory oxides based on adding indium oxide to rare earth-stabilized hafnium oxide are being studied. The use of indium oxide generally increases the electrical conductivity. The results of measurements of the electrical conductivity and data on corrosion resistance in molten salts are presented.

INTRODUCTION

Electrically conducting refractory oxides are being studied at Pacific Northwest Laboratory (PNL) for use in magnetohydrodynamic (MHD) generators, fuel cells, and thermoelectric generators. Each of these uses requires ceramics with adequate electrical conductivity. For use in MHD generators and fuel cells, the ceramics also need to be resistant to chemical and electrochemical corrosion. In some of the applications, the electrical conductivity must be adequate over a wide temperature range from near room temperature and above. Since ceramics generally exhibit a decrease in electrical conductivity as the temperature decreases, composites of two or more compositions may be necessary to assure adequate conductivity over a wide temperature range. Composite electrodes have been fabricated (Marchant and Bates 1982) using a rare earth-stabilized hafnium oxide composition for the high-temperature component and a rare earth-stabilized hafnium oxide-indium oxide composition for the low-temperature component.

This paper focuses on the properties of the lower temperature component containing indium oxide. The results of electrical conductivity and corrosion tests are reported.

EXPERIMENTAL PROCEDURES

Powder Preparation and Fabrication

All samples used in the property measurements were prepared by sintering coprecipitated powders. The coprecipitation technique was a modification of that used by Dole et al. (1978). The rare earth oxides and indium oxides were dissolved in hot nitric acid. The hafnium oxychloride was dissolved in water.

(a) Operated for the U.S. Department of Energy by Battelle Memorial Institute.

The solutions were mixed and diluted with distilled water to about 10 times the volume. The resulting solution was slowly dripped into dilute ammonium hydroxide to coprecipitate the powder. The final pH was adjusted to between 8.0 and 8.5 to ensure complete precipitation.

The resulting precipitate was washed sequentially with water, acetone, toluene, and acetone, then air dried. The powder was screened through a -20 mesh Tyler sieve[a] to granulate, then calcined at 1073K for 4 h. The resulting powder had a surface area ranging between 5 and 25 m^2/g (BET equation using argon). The powder was then ball milled for 16 h in a neoprene-lined ball mill using zirconia balls and Freon® liquid.

The powder was compacted into a rectangular bar using cold pressing in steel dies and isostatic pressing, then sintered at temperatures between 1800K and 1850K for 20 h. The sintered bars were cut to the shapes needed for testing using a diamond saw.

Electrical Conductivity

The electrical conductivity was measured to 1700K in air using a four-contact direct-current method. A rectangular-shaped sample with a square cross section was mounted on platinum supports. Platinum paste was used to provide better contact between the support and the sample. Platinum knife edges were used as the electric potential probes. Direct electric current (current densities not exceeding 0.05 amp/cm^2) was passed through the samples, and the electric potential between the two knife-edge probes was measured. No polarization was observed during the measurements on most of the highly conducting ceramics .

Corrosion

The corrosion tests consisted of immersing the rectangular test samples in the molten salt for a predetermined time. The samples were removed and cooled; the surface molten salt was removed by washing in a dilute nitric acid. The dimensions of the samples were measured, and the samples were either reimmersed in the molten salt or sent to metallography for cross-sectional polishing and examination. All testing was done in an air atmosphere. The molten salts were prepared by melting powders of the perspective salts in an alumina crucible. Two molten salt solutions were used: 1) K_2SO_4 and 2) 0.62 Li_2CO_3·0.38 K_2CO_3.

(a) Use of manufacturer names does not imply PNL endorsement.
® Trademark of E. I. du Pont de Nemours and Company, Inc., Wilmington, Delaware.

RESULTS AND DISCUSSION

Electrical Conductivity

The electrical conductivities of several compositions with different indium oxide contents are shown in Figure 1. The compositions of the samples in Figure 1 are given in Table 1 along with the equations used to generate the lines representing least squares fits to the data. Praseodymium oxide is the major rare earth component. In the chemical formulations, the nonstoichiometric praseodymium oxide is represented as PrO_2, although the starting powder prior to coprecipitation was Pr_6O_{11}. The conductivity for pure In_2O_3 is included in the figure. The electrical conductivity increases with increasing amounts of In_2O_3. The activation energies used to describe the temperature dependence of the conductivity are also included in the table. As expected, the high-temperature activation energies are greater than those for the low-temperature conductivity. The low-temperature activation energy generally decreases with the increased In_2O_3 content.

Three of these compositions were examined with the scanning electron microscope (SEM/EDX) and x-ray diffraction (XRD); the results are given in Table 2. The phase that appears to result in the higher conductivity is the body-centered-cubic (BCC) phase, which is an In_2O_3-type structure. The SEM/EDX analysis shows that the In_2O_3 phase contains substantial amounts of the other constituents. In general, the more In_2O_3 added to the material, the greater the amount of the BCC phase and the higher the electrical conductivity.

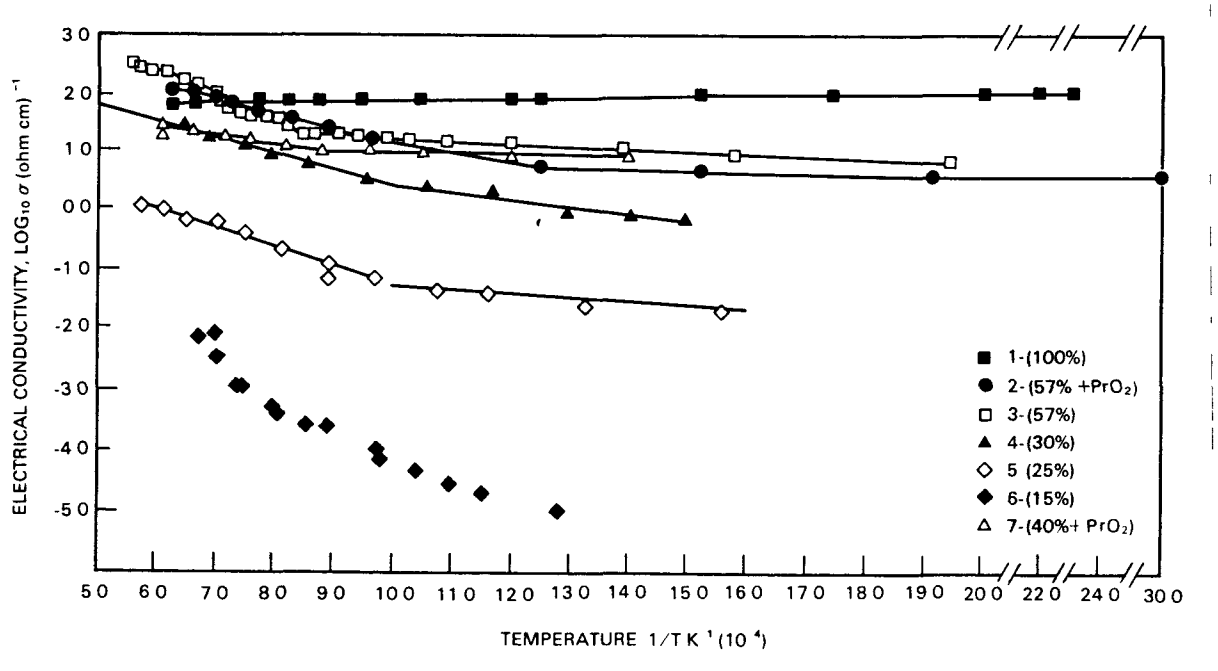

FIGURE 1. Electrical Conductivity of Several Samples; Compositions Given in Table 1. The amount of In_2O_3 in mol% for each sample is shown in parentheses.

TABLE 1. Compositions of Samples Shown in Figure 1

Sample Number	Composition, mol%	$Log_{10}\sigma$ = (ohm^{-1} cm^{-1})	Activation Energy, eV	Temperature Range, K
1	In_2O_3	$1.7519 + 1.5607 \times 10^2\ K^{-1}$	-0.03	397 to 1631
2	0.57 In_2O_3•0.43 ( )[a]	$1.138 - 2.544 \times 10^2\ K^{-1}$	0.05	335 to 930
		$3.878 - 2.783 \times 10^3\ K^{-1}$	0.55	987 to 1647
3	0.57 In_2O_3•0.43 [ ][b]	$1.6601 - 4.425 \times 10^2\ K^{-1}$	0.09	1781 to 1064
		$4.6644 - 3.846 \times 10^3\ K^{-1}$	0.76	513 to 1101
4	0.30 In_2O_3•0.70 [ ][b]	$3.4708 - 1.123 \times 10^3\ K^{-1}$	0.27	1052 to 1551
		$5.5295 - 3.325 \times 10^3\ K^{-1}$	0.66	851 to 1052
5	0.25 In_2O_3•0.75 [ ][b]	$0.4468 - 8.118 \times 10^2\ K^{-1}$	0.16	645 to 933
		$1.9582 - 3.177 \times 10^3\ K^{-1}$	0.63	1031 to 1727
6	0.15 In_2O_3•0.85 [ ][b]	(c)	(c)	(c)
7	0.40 In_2O_3•0.60 ( )[a]	(d)	(d)	525 to 1105
		$2.1771 - 1.328 \times 10^3\ K^{-1}$	0.26	1135 to 1688

(a)( ) = (35.8 mol% PrO_2•6.0 mol% Yb_2O_3•58.8 mol% HfO_2).
(b)[ ] = [28.6 mol% PrO_2•4.8 mol% Yb_2O_3•66.6 mol% HfO_2].
(c) Not linear.
(d) Nearly temperature independent.

TABLE 2. Results of XRD and SEM/EDX Analyses for Three Compositions (see Figure 1)

Sample Number[a]	XRD Relative Amount	SEM/EDX, mol% In_2O_3	PrO_2	Yb_2O_3	HfO_2
3. 0.57 In_2O_3•0.43( )	Major BCC[b] In_2O_3-type structure a_o = 10.130 Å(c)	79	7	2	12
	Minor FCC fluorite HfO_2-type structure a_o = 5.18 Å(d)	9	32	4	55
5. 0.30 In_2O_3•0.70[ ]	Equal BCC In_2O_3-type structure a_o = 10.135 Å	52	14	3	31
	Equal FCC fluorite HfO_2-type structure a_o = 5.15 Å	24	19	4	53
7. 0.15 In_2O_3•0.85[ ]	Major FCC fluorite hafnium-type structure a_o = 5.17 Å	11	28	5	56
	Minor BCC In_2O_3-type structure a_o = 10.2 Å	74	3	15	8

(a) See Table 1 for nomenclature identification.
(b) BCC = body-centered cubic
FCC = face-centered cubic.
(c) Pure In_2O_3; a_o = 10.118 A.
(d) Pure HfO_2; a_o = 5.10 A.

This conclusion appears to be generally consistent with all the data that have been examined. Occasionally a sample exhibited higher conductivity than expected for the amount of In_2O_3 (Sample 8 of Figure 1). These samples usually contained a higher concentration of In_2O_3 in the In_2O_3 phase or a greater amount of face-centered-cubic PrO_2 solid solution phase. This solid solution phase is not listed for the three compositions in Table 2 but was found in Sample 8 (Table 1). The phase had a lattice parameter of around 5.33 Å. The composition has not yet been determined.

One of the compositions (Sample 5, Table 1) was examined using the transmission electron microscope to determine the extent of grain boundary concentration of the In_2O_3-containing phase. A typical area is shown in Figure 2.

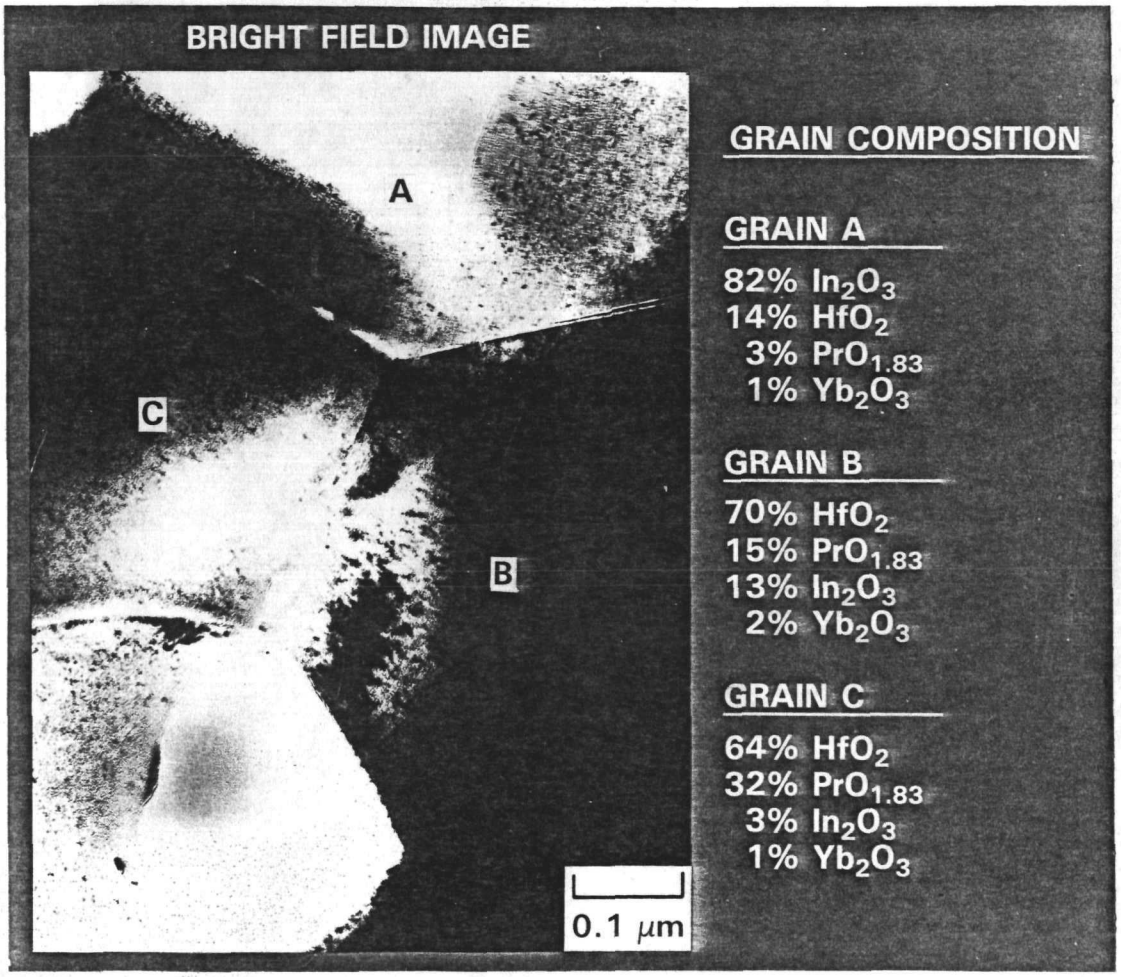

FIGURE 2. Microstructure and Microchemistry of Sample 5 (Table 1)

The compositions of the grains shown in the figure are representative of other areas. No higher concentration of In_2O_3 was found along the grain boundaries nor were additional phases found along the boundaries except at some triple points and in isolated areas. The electrical conductivity at the grain boundaries may still be extensive due to additional defects and unmeasurable concentrations of impurities. The grains were also examined with electron diffraction to determine the crystal structure. The results are given in Figure 3. The pyrochlore phase identified with electron diffraction was not observed with XRD, probably because the concentration was quite low since only a few grains of pyrochlore were found after examining several areas. The other two phases were found with XRD as shown in Table 2.

Initially, the compositions were formulated to obtain some pyrochlore as predicted by Kravchinskaya et al. (1978) for the binary HfO_2-Pr_2O_3. The large amounts of In_2O_3 appeared to override the pyrochlore formation. Although phase equilibria are not currently available on the HfO_2-PrO_2-In_2O_3 ternary, data are available for the ternary ZrO_2-Y_2O_3-In_2O_3 (Schusterius and Padurow 1953). Even though ZrO_2 and HfO_2 have very closely related properties, Y_2O_3 and PrO_2 do not; consequently, the phase equilibria are not directly applicable. The phase equilibria did show that the In_2O_3-ZrO_2 binary had the following: 1) monoclinic ZrO_2 from 0 to 3 mol% In_2O_3; 2) two-phase region between 3 and 9 mol% In_2O_3; 3) a face-centered-cubic structure from 9 to 22 mol% In_2O_3; 4) a miscibility gap from 22 to 95 mol% In_2O_3; and 5) a body-centered-cubic lattice from 95 to 100% In_2O_3. Adding Y_2O_3 to the binary decreased the concentration range of the miscibility gap.

Most of the ternary HfO_2 compounds described in this paper are multiphase, including both a face-centered cubic and a body-centered cubic. Therefore, a miscibility gap may occur with the compositions of the two phases partially determined by the amount of PrO_2 present. Further work is being conducted to determine the phase equilibria.

Corrosion Testing

Corrosion testing is currently being conducted on several of the previously mentioned materials in both molten 0.62 Li_2CO_3•0.38 K_2CO_3 at 923K and K_2SO_4 at 1373K. Results are available for only two of the compositions in Table 1. The first is the pure In_2O_3. After immersion in the molten Li_2CO_3-K_2CO_3 solution for 1792 h, the corrosion rate was about 4×10^{-5} g/cm^2-h. Binary compositions tested for the same length of time had lower corrosion rates, i.e., 0.50 In_2O_3•0.50 HfO_2, 0.30 In_2O_3•0.70 HfO_2, 0.45 In_2O_3•0.55 HfO_2, and 0.40 In_2O_3•0.60 HfO_2 all had corrosion rates of about 2×10^{-6} g/cm^2-h, which is the lower limit of measurement for the tests. Each of these corrosion samples tended to show In_2O_3 loss, but the corrosion rates of the In_2O_3 compounds were significantly less than pure In_2O_3, probably due to both the dilution with HfO_2 and the formation of compounds.

Sample 3 from Table 1 was corrosion tested in molten K_2SO_4 at 1373K for 168.5 h. The density was 5.37 g/cm^3, which is approximately 70% of theoretical. Most of the porosity was interconnected, resulting in the filling of the porosity with K_2SO_4 during the corrosion test. The corrosion rate was about

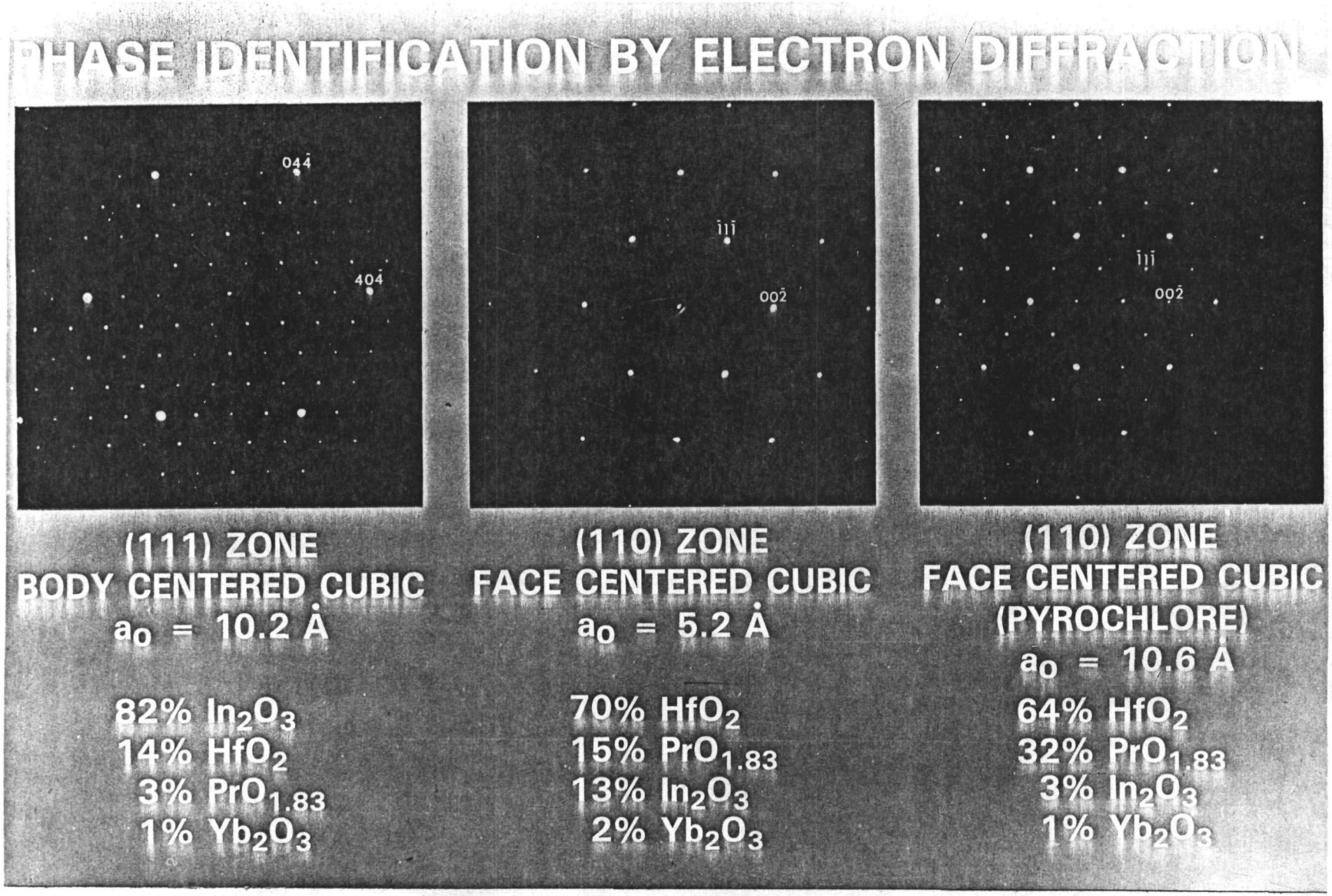

FIGURE 3. Crystal Structure Determined by Electron Diffractions of Sample 5 from Table 2

3×10^{-5} g/cm^2-h, which was close to the limits of the test. Potassium had diffused into some of the grains and was detected by the SEM/EDX. Sulfur was not detected in the grain; consequently, sulfur does not appear to interact with the solid but remains with the potassium in the K_2SO_4 melt. Some selective corrosion of In_2O_3 occurred since the molten salt had a higher concentration of In_2O_3 than expected from uniform corrosion.

CONCLUSIONS

Ceramic oxides with high electrical conductivity have been prepared by adding indium oxide to rare earth-stabilized hafnium oxides. Generally, indium oxide additions greater than 15 mol% are required to obtain the high electrical conductivity. The indium oxide is especially effective for increasing the low-temperature electrical conductivity. The corrosion in lithium carbonate-potassium carbonate melts and molten potassium sulfate appears to favor the dissolution of indium oxide. The compounding of indium oxide with the rare earth hafnates yielded lower corrosion rates than pure indium oxide.

REFERENCES

Dole, S. L., et al. 1978. "Technique for Preparing Highly Sinterable Oxide Powders." Materials Science and Engineering, 32:277-281.

Kravchinskaya, M. V., et al. 1978. "Phase Diagrams of the Systems HfO_2-Pr_2O_3 and Dy_2O_3-Pr_2O_3." Ceramurgia International, 4:14-17.

Schusterius, C., and N. N. Padurow. 1953. "Isomorphiebeziehungen In System In_2O_3-Y_2O_3-ZrO_2." Ber. Deut. Ker. Ges., 30:235-239.

Marchant, D. D., and J. L. Bates. 1982. "Development and Testing of Hafnium Oxide-Based MHD Electrodes." In 20th Symposium on the Engineering Aspects of Magnetohydrodynamics, ed. J. A. Hardgrove, pp. 11.4.1-11.4.5, University of California, Irvine, California.